Two-magnon contribution to the ferromagnetic resonance linewidth in amorphous ferromagnetic metals

J. F. Cochran, R. W. Qiao, and B. Heinrich
Department of Physics, Simon Fraser University, Burnaby, British Columbia, Canada V5A 1S6
(Received 21 September 1988)

The wave-number- and frequency-dependent susceptibility $\chi(k,\omega)$ for a ferromagnet in the presence of two-magnon scattering processes, and including intrinsic damping of the Gilbert form, has been calculated using first-order perturbation theory. A simple model was used for the two-magnon scattering: driven magnons of wave vector $\mathbf{k}$ and frequency ω were assumed to be scattered only into states $\mathbf{k}_l$ for which $|\mathbf{k}-\mathbf{k}_l|\leq Q$. The susceptibility $\chi(\mathbf{k},\omega)$ was used to calculate the surface impedance of the metal, and hence to obtain the magnetic field dependence of the absorption of microwave radiation. The theory is expected to be valid for those cases in which the line broadening due to two-magnon scattering is small compared with the line broadening due to intrinsic processes. A numerical calculation was carried out using magnetic parameters appropriate for the amorphous ferromagnet $Fe_{82}B_{18}$. The two-magnon scattering contributed an amount to the linewidth which varied slowly with frequency. Thus the two-magnon scattering mechanism may be the origin of the nearly frequency-independent ferromagnetic resonance line broadening which has been observed for many amorphous metallic ferromagnets.

I. INTRODUCTION

The ferromagnetic resonance (FMR) absorption linewidth observed for metals is a complex function of frequency because of exchange-conductivity effects.[1,2] Intrinsic magnetic damping can be represented in the Landau-Lifshitz equations of motion for the magnetization by an effective field which is proportional to frequency, $H_d=(\omega/\gamma)(G/\gamma M_s)$, where G is the Gilbert damping parameter.[3] The exchange-conductivity contribution to the linewidth varies as $\omega^{1/2}$ for a metal for which it is appropriate to use a local conductivity, i.e., one for which $\mathbf{j}=\sigma\boldsymbol{\epsilon}$. For sufficiently large frequencies the FMR linewidth is dominated, therefore, by the term proportional to the frequency. A calculation[3] using the Landau-Lifshitz equations, the Rado-Weertman general exchange boundary conditions, and Maxwell's equations shows that in this high-frequency limit the linewidth can be represented by

$$\Delta H=\Delta H(0)+\beta\left[\frac{G}{\gamma M_s}\right]\left[\frac{\omega}{\gamma}\right]. \tag{1}$$

For a homogeneous metal, the zero frequency intercept $\Delta H(0)$ is expected to be quite small—of the order of a few Oersteds; it is a consequence of exchange-conductivity broadening. The parameter β, of order 1, depends to some extent on the material and upon the degree of pinning at the surface of the ferromagnet. For unpinned spins $\beta\simeq 1.5$; for fully pinned spins $\beta\simeq 1.6$. A considerable body of data has been reported for amorphous metallic ferromagnets[4-11] for which the FMR linewidth was found to depend linearly on frequency, but for which the zero frequency offset was much larger than that calculated using a value for the intrinsic damping parameter derived from the slope of ΔH versus frequency. Similar effects have been observed in thin films for which the exchange-conductivity line broadening mechanism could be neglected because the films were thinner than the skin depth.[12-15] It was suggested by Berteaud and Pascard[16] that the excess damping observed in thin films might be due to two-magnon scattering; a damping mechanism which has been found to be important for insulating ferromagnets. The theory of two-magnon scattering has been extensively developed for insulators.[17-19] We wished to extend the theory to include the case of a metal in order to test the hypothesis that the excess zero frequency FMR linewidth offset, $\Delta H(0)$, observed for amorphous ferromagnets could be a consequence of two-magnon scattering due to magnetic inhomogeneities on a submicrometer scale.

At FMR the magnetization in an insulator is driven in the uniform mode, i.e., the wave vector of the magnon which is excited by the incident microwave radiation has the value $q=0$. The theory of inhomogeneity scattering is, therefore, concerned with a scattering event in which a magnon of frequency ω and wave vector $q=0$ is scattered into a magnon having the same frequency, ω, but a different wave vector, $q\neq 0$. It is only necessary to calculate the effect of the two-magnon scattering on the $q=0$ susceptibility, $\chi(\omega,0)$, in order to obtain the fraction of the incident energy absorbed in the ferromagnet near resonance. In a ferromagnetic metal there is no uniform mode because of the finite conductivity which leads to a skin depth δ of order 0.1 μm at a typical experimental frequency of a few GHz. The applied rf field excites magnons in a ferromagnetic metal having a range of wave numbers centered around $q\sim 1/\delta\sim 10^5$ cm^{-1}: it is these magnons which contribute to the absorption of energy from the rf driving field and therefore it is necessary to investigate the effect of two-magnon scattering on magnons having the frequency ω and wave numbers contained within a broad range from $q \sim 0$ to $q \sim 10^6$ cm^{-1}. In order to obtain the absorption it is necessary to know the wave-number-dependent susceptibility $\chi(\omega,q)$ over the above range. This $\chi(\omega,q)$ can then be used, together with Maxwell's equations and suitable boundary conditions, to calculate the rate of energy absorbed from the incident microwave field.[20]

In our calculations we have taken full account of the ellipticity of the precessing magnons because we are interested in the parallel configuration in which the static magnetization and the applied magnetic field lie in the plane of a semi-infinite slab, Fig. 1. This ellipticity enormously complicates the susceptibility calculation. However, for the parallel geometry the ratio of the transverse magnetization components at FMR, $|m_x/m_y| \approx (B/H)^{1/2}$, becomes large at low frequencies for iron-based alloys which have a large static magnetization. For example, for $4\pi M_s = 16$ kOe, and for $\omega/\gamma = 3$ kOe corresponding to a frequency of 10 GHz, this ellipticity is 5.4. A simplified treatment of two-magnon scattering in metals has been presented previously.[21]

II. TWO-MAGNON SCATTERING

The susceptibility for the magnetic metal will be calculated for the Hamiltonian

$$H = H_o + H_2 \, , \tag{2}$$

where H_o is the usual Holstein-Primakoff Hamiltonian (Sparks,[18] Chap. 3):

$$H_o = \hbar\gamma \sum_q A_q b_q^\dagger b_q + \frac{\hbar\gamma}{2} \sum_q (B_q b_q b_{-q} + B_q^* b_{-q}^\dagger b_q^\dagger) \, . \tag{3}$$

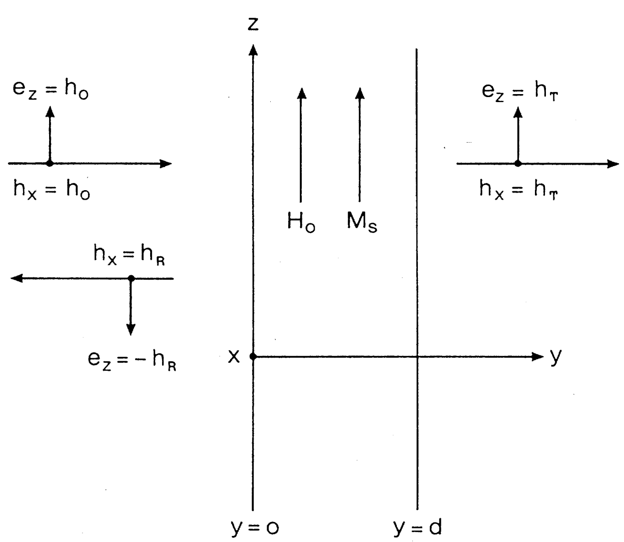

FIG. 1. The geometry used to calculate the surface impedance of a semi-infinite slab of metal, having thickness d, and having its surface lying in the x-y plane. The applied field, H_o, and the static magnetization, M_s, are directed along the z axis. Microwave radiation of amplitude h_o is incident from the left. The amplitudes of the reflected and transmitted microwave radiation are h_R and h_T.

$b_q^\dagger, b_q$ are creation and annihilation operators for quantized spin waves (magnons) which obey the commutation rules

$$b_q b_{q'}^\dagger - b_{q'}^\dagger, b_q = \delta_{qq'} \; ; \tag{4}$$

all other commutators are zero. The constants A_q, B_q are given by

$$A_q = A_{-q} = H + 2\pi M_s \sin^2\theta_q + \frac{2A}{M_s} q^2 \, , \tag{5a}$$

$$B_q = B_{-q} = 2\pi M_s \sin^2\theta_q e^{-2i\phi_q} \, , \tag{5b}$$

where H is the static magnetic field applied along the z axis in the plane of a thin disc-shaped specimen whose demagnetizing coefficients for fields in the plane are negligibly small (see Fig. 1). The saturation magnetization M_s is parallel with the static field. The wave vector q which characterizes the magnon propagation is described by the polar angles θ_q, ϕ_q where $q_x = q \sin\theta_q \cos\phi_q$ and $q_z = q \cos\theta_q$. The magnetization components are given in terms of magnon operators by (Turov[22])

$$m_+(\mathbf{r}) = \left[\frac{2\hbar\gamma M_s}{V} \right]^{1/2} \sum_q e^{-i\mathbf{q}\cdot\mathbf{r}} b_q^\dagger \, , \tag{6a}$$

$$m_-(\mathbf{r}) = \left[\frac{2\hbar\gamma M_s}{V} \right]^{1/2} \sum_q e^{+i\mathbf{q}\cdot\mathbf{r}} b_q \, , \tag{6b}$$

where

$$m_+ = m_x + i m_y \tag{7a}$$

and

$$m_- = m_x - i m_y \, . \tag{7b}$$

Also,

$$m_z(\mathbf{r}) = M_s - \frac{\gamma\hbar}{V} \sum_{q,q'} e^{i(\mathbf{q}-\mathbf{q}')\cdot\mathbf{r}} b_{q'}^\dagger b_q \, . \tag{7c}$$

In the above expressions, V is the volume of the specimen. The scattering Hamiltonian H_2 is assumed to have the form

$$H_2 = \hbar\gamma \sum_{\substack{m,l \\ m \neq l}} \left[F_{m,l} b_m^\dagger b_l + \frac{R_{m,l}}{2} b_{-m}^\dagger b_l^\dagger + \frac{R_{m,l}^*}{2} b_{-m} b_l \right] , \tag{8}$$

where

$$F_{l,m}^* = F_{m,l} \, .$$

We shall consider scattering due to a small volume within which the exchange stiffness deviates from the average, or within which the anisotropy constants or the magnetization deviate from the average value. Kopsky[23] has treated exchange and anisotropy scattering from small clusters; Sparks, Loudon, and Kittel[24] have discussed two-magnon scattering due to magnetization inhomogeneities; and Schmidt[25] has discussed scattering from the strain field near a dislocation.

A. Exchange scattering

For a single small region of volume v_α, Kopsky[23] has shown that the scattering Hamiltonian can be written in the form of Eq. (8) with

$$F_{m,l}^{\alpha}=\mathbf{k}_l\cdot\mathbf{k}_m\left[\frac{2\Delta A_\alpha}{M_s}\right]e^{i(\mathbf{k}_l-\mathbf{k}_m)\cdot\mathbf{R}_\alpha}\times\left[\frac{1}{V}\int_{v_\alpha}e^{i(\mathbf{k}_l-\mathbf{k}_m)\cdot\rho}d^3\rho\right],$$

$$R_{m,l}=R_{m,l}^{*}=0\ .$$

In this equation ΔA_α is the amount by which the exchange stiffness in the scattering volume, v_α, deviates from that for the matrix material, and $\mathbf{R}_\alpha$ is the position vector for the imperfection centroid. Notice that the effective volume

$$v_{m,l}^{\alpha}=\int_{v_\alpha}e^{i(\mathbf{k}_l-\mathbf{k}_m)\cdot\rho}d^3\rho$$

introduces a natural cutoff wave vector Q, which is related to the dimensions of the imperfection. For a spherical imperfection of radius R one has $Q\sim 2\pi/R$, and for $|\mathbf{k}_l-\mathbf{k}_m|\gg Q$ the effective scattering volume becomes negligibly small. It is assumed that the contributions from individual scattering centers are additive:

$$F_{m,l}=\mathbf{k}_l\cdot\mathbf{k}_m\sum_\alpha\left[\frac{2\Delta A_\alpha}{M_s}\right]e^{i(\mathbf{k}_l-\mathbf{k}_m)\cdot\mathbf{R}_\alpha}\left[\frac{v_{m,l}^{\alpha}}{V}\right]. \quad (9)$$

B. Anisotropy scattering

For this case Kopsky[23] has shown that

$$F_{m,l}=\frac{2\Delta K}{M_s}\sum_\alpha e^{i(\mathbf{k}_l-\mathbf{k}_m)\cdot\mathbf{R}_\alpha}\left[\frac{v_{m,l}^{\alpha}}{V}\right]A_{\mathrm{an}}^{\alpha}\ , \quad (10a)$$

$$R_{m,l}=\frac{2\Delta K}{M_s}\sum_\alpha e^{-i(\mathbf{k}_l-\mathbf{k}_m)\cdot\mathbf{R}_\alpha}\left[\frac{v_{m,l}^{\alpha}}{V}\right]B_{\mathrm{an}}^{\alpha}\ , \quad (10b)$$

where, as above, $v_{m,l}^{\alpha}$ is an effective volume, and $\mathbf{R}_\alpha$ specifies the location of the inhomogeneity. Both A_{an}^{α} and B_{an}^{α} are complicated functions of the angles which specify the directions of the anisotropy axes in the inhomogeneity relative to the specimen axes. Their precise form is of no interest since no attempt will be made to calculate the scattering amplitudes from the first principles.

C. Scattering due to magnetization inhomogeneities

Following Sparks, Loudon, and Kittel[24] the scattering amplitudes for a very small volume element whose radius R is small compared with the magnon wavelength, i.e., $k_lR\ll 1$, can be written

$$F_{m,l}\approx 3\pi\left[\frac{(4\pi/3)R^3}{V}\right](\Delta M_s)(3\cos^2\theta_m-1)\times\sum_\alpha e^{i(k_l-k_m)\cdot\mathbf{R}_\alpha}\ ,$$

$$R_{m,l}=0\ . \quad (11)$$

The scattering amplitudes will be used in a first-order perturbation calculation in which products of these amplitudes are encountered. It is taken as a postulate that the scattering centers are randomly distributed so that waves which have been scattered from the imperfection at $\mathbf{R}_\alpha$ do not add coherently to waves which have been scattered from the imperfection at $\mathbf{R}_\beta$. Consequently, terms in the perturbation expansion such as $|F_{m,l}|^2$ give a contribution which is proportional to the number of scattering centers; cross terms in the product series average to zero. Similarly, products of $F_{i,j}$ and $R_{m,l}$ are postulated to be vanishingly small except when $i=m$ and $j=l$. These postulates are equivalent to the postulated random phase of the Fourier components of the scattering amplitude which was used by Schlömann[19] in his discussion of two-magnon scattering in insulating ferromagnets.

III. THE WAVE-NUMBER- AND FREQUENCY-DEPENDENT SUSCEPTIBILITY

We wish to calculate the magnetic response of the system specified by the Hamiltonian (2) to a small driving field having unit amplitude, polarized perpendicular to the static field (along x, see Fig. 1), and propagating along the specimen normal:

$$h_x=e^{i(ky-\omega t)}\ . \quad (12)$$

The resulting magnetizations are given[26] by

$$\langle m_x\rangle=-\tfrac{1}{2}(\hbar\gamma M_s)\sum_q\Big[e^{i\mathbf{q}\cdot\mathbf{r}}[G_1(q)+G_2(q)]+e^{-i\mathbf{q}\cdot\mathbf{r}}[G_3(q)+G_4(q)]\Big]\ , \quad (13a)$$

$$\langle m_y\rangle=-\frac{i}{2}(\hbar\gamma M_s)\sum_q\Big[e^{i\mathbf{q}\cdot\mathbf{r}}[G_1(q)+G_2(q)]-e^{-i\mathbf{q}\cdot\mathbf{r}}[G_3(q)+G_4(q)]\Big]\ , \quad (13b)$$

where

$$G_1(q)=\langle\langle[b_q,b_k^{\dagger}]\rangle\rangle \quad (14a)$$

is 2π times the Fourier transform at frequency $-\omega$ of the retarded Green's function

$$G_1(q,t)=-\frac{i}{\hbar}\Theta(t)\,\mathrm{Tr}[\rho_0(b_q(t),b_k^{\dagger}(o))]\ .$$

The square brackets indicate the commutator of the two operators, ρ_o is the equilibrium density operator, and

$\Theta(t)$ is the unit step function. Similarly,

$$G_2(q)=\langle\langle [b_q,b_{-k}]\rangle\rangle \ , \tag{14b}$$

$$G_3(q)=\langle\langle [b_q^\dagger,b_{-k}]\rangle\rangle \ , \tag{14c}$$

$$G_4(q)=\langle\langle [b_q^\dagger,b_k^\dagger]\rangle\rangle \ . \tag{14d}$$

The Green's functions (14) are related to the response of the system to circularly polarized driving fields. For example, $G_1(q)$ and $G_4(q)$ are proportional to the responses $\langle m_-(q)\rangle$ and $\langle m_+(q)\rangle$ generated by the driving field $h_-(k)=h_x-ih_y$. Similarly, $G_2(q)$ and $G_3(q)$ are proportional to the responses $\langle m_-(q)\rangle$ and $\langle m_+(q)\rangle$ generated by the driving field $h_+(k)=h_x+ih_y$. Because of magnetic dipole-dipole interactions, the precession of the magnetization is elliptically polarized so that a circularly polarized driving field generates both left- and right-handed circularly polarized components. The Green's functions (14) satisfy the following equations of motion:[26]

$$\hbar(\omega+i\epsilon)G_1(q)=\delta_{q,k}+\langle\langle [[b_q,H],b_k^\dagger]\rangle\rangle \ , \tag{15a}$$

$$\hbar(\omega+i\epsilon)G_2(q)=\langle\langle [[b_q,H],b_{-k}]\rangle\rangle \ , \tag{15b}$$

$$\hbar(\omega+i\epsilon)G_3(q)=-\delta_{q,-k}+\langle\langle [[b_q^\dagger,H],b_{-k}]\rangle\rangle \ , \tag{15c}$$

$$\hbar(\omega+i\epsilon)G_4(q)=\langle\langle [[b_q^\dagger,H],b_k^\dagger]\rangle\rangle \ . \tag{15d}$$

The quantity ϵ is a small, positive infinitesimal which is required to ensure that the impulse response goes to zero at very large times after the application of the impulse.

Using the Hamiltonian (2), one obtains

$$\hbar\gamma V_q^- G_1(q)=\delta_{q,k}+\hbar\gamma B_q^* G_4(-q) +\hbar\gamma \sum_{l\neq q} F_{q,l}G_1(l)+\hbar\gamma \sum_{l\neq -q} R_{-q,l}G_4(l) \ , \tag{16a}$$

$$V_q^- G_2(q)=B_q^* G_3(-q)+\sum_{l\neq q} F_{q,l}G_2(l) + \sum_{l\neq -q} R_{-q,l}G_3(l) \ , \tag{16b}$$

$$\hbar\gamma V_q^+ G_3(q)=-\delta_{q,-k}-\hbar\gamma B_q G_2(-q) -\hbar\gamma \sum_{l\neq q} F_{q,l}^* G_3(l)-\hbar\gamma \sum_{l\neq -q} R_{-q,l}^* G_2(l) \ , \tag{16c}$$

$$V_q^+ G_4(q)=-B_q G_1(-q)-\sum_{l\neq q} F_{q,l}^* G_4(l) - \sum_{l\neq -q} R_{-q,l}^* G_1(l) \ , \tag{16d}$$

where, for compactness, we have introduced the notation

$$V_q^\pm=\left[\frac{\omega+i\epsilon}{\gamma}\right]\pm A_q \ . \tag{17}$$

In the absence of two-magnon scattering, the only nonzero Green's functions are given by

$$G_1(k)=v_k^+/\hbar\gamma D_k \ , \tag{18a}$$

$$G_2(k)=-B_k^*/\hbar\gamma D_k \ , \tag{18b}$$

$$G_3(-k)=-v_k^-/\hbar\gamma D_k \ , \tag{18c}$$

$$G_4(-k)=-B_k/\hbar\gamma D_k \ , \tag{18d}$$

where

$$D_k=v_k^+v_k^-+|B_k|^2 = \left[\frac{\omega+i\epsilon}{\gamma}\right]^2-\left[H+4\pi M_s \sin^2\theta_k+\frac{2Ak^2}{M_s}\right] \times\left[H+\frac{2Ak^2}{M_s}\right] . \tag{19}$$

Intrinsic magnetic damping can be taken into account by replacing the magnetic field H, wherever it occurs, by the combination

$$\left[H-\left[\frac{i\omega}{\gamma}\right]\left[\frac{G}{\gamma M_s}\right]\right] . \tag{20}$$

This can be shown by comparing the expressions for the magnetization components obtained from (13), and using the Green's functions (18), with magnetizations calculated from the Landau-Lifshitz equations of motion including a damping term having the Gilbert form.

The set of coupled equations (16) cannot be solved exactly. We have carried through a perturbation calculation in which the first-order Green's functions (18) are used to estimate a first approximation for those Green's functions which vanish in the limit of no two-magnon scattering. The new first-order Green's functions were used to calculate $G_1(k)$, $G_2(k)$, $G_3(-k)$, and $G_4(-k)$ correct to second order. The algebra involved is very tedious. The result is

$$G_1(k)=\frac{\langle V_k^+\rangle}{\hbar\gamma\langle D_k\rangle} \ , \tag{21a}$$

$$G_2(k)=\frac{-\langle B_k\rangle^*}{\hbar\gamma\langle D_k\rangle} \ , \tag{21b}$$

$$G_3(-k)=\frac{-\langle V_k^-\rangle}{\hbar\gamma\langle D_k\rangle} \ , \tag{21c}$$

$$G_4(-k)=\frac{-\langle B_k\rangle}{\hbar\gamma\langle D_k\rangle} \ , \tag{21d}$$

where

$$\langle V_k^-\rangle=V_k^-+\sum_{l\neq k}\frac{(V_l^-|R_{k,l}|^2-V_l^+|F_{k,l}|^2+B_lF_{k,l}^*R_{k,l}^*+B_l^*F_{k,l}R_{k,l})}{D_l} \ , \tag{22a}$$

$$\langle V_k^+ \rangle = V_k^+ + \sum_{l \neq k} \frac{(V_l^+ |R_{k,l}|^2 - V_l^- |F_{k,l}|^2 - B_l F_{k,l} R_{k,l} - B_l^* F_{k,l}^* R_{k,l}^*)}{D_l} , \tag{22b}$$

$$\langle B_k \rangle = B_k + \sum_{l \neq k} \frac{(V_l^+ F_{k,l}^* R_{k,l}^* - V_l^- F_{k,l} R_{k,l} - B_l |F_{k,l}|^2 - B_l^* |R_{k,l}|^2)}{D_l} , \tag{22c}$$

$$\langle D_k \rangle = \langle V_k^- \rangle \langle V_k^+ \rangle + |\langle B_k \rangle|^2 . \tag{22d}$$

Recall that

$$V_l^{\pm} = \left[\frac{\omega}{\gamma} \right] \pm A_l , \tag{23a}$$

$$A_l = H - i \left[\frac{\omega}{\gamma} \right] \left[\frac{G}{\gamma M_s} \right] + 2\pi M_s \sin^2\theta_l + \frac{2A}{M_s} k_l^2 , \tag{23b}$$

$$B_l = 2\pi M_s \sin^2\theta_l e^{-2i\phi_l} , \tag{23c}$$

$$\begin{aligned} D_l &= V_l^- V_l^+ + |B_l|^2 \\ &= \left[\frac{\omega}{\gamma} \right]^2 - \left[H + 4\pi M_s \sin^2\theta_l + \frac{2A}{M_s} k_l^2 \right. \\ &\qquad \left. - \left[\frac{i\omega}{\gamma} \right] \left[\frac{G}{\gamma M_s} \right] \right] \\ &\qquad \times \left[H + \frac{2A}{M_s} k_l^2 - \left[\frac{i\omega}{\gamma} \right] \left[\frac{G}{\gamma M_s} \right] \right] . \end{aligned} \tag{23d}$$

The Green's functions (21) can be used to calculate the magnetizations from Eqs. (13). Since these magnetizations are the response to a unit driving field polarized along the x direction, they are also the susceptibilities required for the solution of the electromagnetic boundary value problem. Explicitly, these susceptibilities are

$$\chi_{xx}(k,\omega) = -\left[\frac{M_s}{2} \right] \left[\frac{\langle V_k^+ \rangle - \langle V_k^- \rangle - \langle B_k \rangle - \langle B_k \rangle^*}{\langle D_k \rangle} \right] , \tag{24a}$$

$$\chi_{yx}(k,\omega) = -i \left[\frac{M_s}{2} \right] \left[\frac{\langle V_k^+ \rangle + \langle V_k^- \rangle + \langle B_k \rangle - \langle B_k \rangle^*}{\langle D_k \rangle} \right] . \tag{24b}$$

These susceptibilities have been calculated using only primary two-magnon scattering processes as defined by Schlömann.[19] That is, the effect of two-magnon scattering on the breadth of the intermediate states k_l in Eqs. (22) has been ignored. This should be an adequate approximation so long as the contribution to the linewidth of a particular state due to intrinsic damping mechanisms, $(\omega/\gamma)(G/\gamma M_s)$, is larger than the two-magnon scattering contribution.

IV. THE SURFACE IMPEDANCE OF THE METAL

For the geometry of Fig. 1, and for an incident microwave field polarized with the electric vector along z, Maxwell's equations for the metal become (for a time dependence $e^{-i\omega t}$)

$$\frac{\partial e_z}{\partial y} = \frac{i\omega}{c} b_x = \frac{i\omega}{c}(h_x + 4\pi m_x) , \tag{25a}$$

$$\frac{\partial h_x}{\partial y} = -\frac{4\pi\sigma}{c} e_z , \tag{25b}$$

$$b_y = 0 . \tag{25c}$$

It has been assumed that the only spatial variation in the metal is along y, the specimen normal; also, the displacement current has been neglected relative to the conduction current σe_z. Because of the nonlocal relationship between the magnetization and the magnetic field, it is useful to expand the rf fields in Fourier series. Let

$$h_x(y) = h_o + \sum_{n=1}^{\infty} h_n \cos\left[\frac{n\pi y}{d} \right] , \tag{26a}$$

$$m_x(y) = \chi_{xx}(o) h_o + \sum_{n=1}^{\infty} \chi_{xx}(n) h_n \cos\left[\frac{n\pi y}{d} \right] , \tag{26b}$$

$$m_y(y) = \chi_{xy}(o) h_o + \sum_{n=1}^{\infty} \chi_{yx}(n) h_n \cos\left[\frac{n\pi y}{d} \right] , \tag{26c}$$

and

$$e_z(y) = \sum_{n=1}^{\infty} e_n \sin\left[\frac{n\pi y}{d} \right] , \tag{26d}$$

where $\chi_{xx}(n)$ and $\chi_{yx}(n)$ are the wave-number- and frequency-dependent susceptibilities from Eqs. (24) evaluated for the wave number $k = n\pi/d$. In Eqs. (26) one has

$$h_o = \frac{1}{d} \int_o^d h_x(y) dy , \tag{27a}$$

$$h_n = \frac{2}{d} \int_o^d h_x(y) \cos\left[\frac{n\pi y}{d} \right] dy , \tag{27b}$$

and

$$e_n = \frac{2}{d} \int_o^d e_z(y) \sin\left[\frac{n\pi y}{d} \right] dy . \tag{27c}$$

Substitution of the series (26) in Maxwell's equations leads to relations between the coefficients e_n and h_n which can be solved to obtain the Fourier amplitudes of the rf magnetic field in terms of the surface electric field values $e_z(o)$ and $e_z(d)$. In particular, the rf magnetic field amplitudes at the slab surfaces, $h_x(o)$ and $h_x(d)$, can be calculated from (26a). A knowledge of the surface values of e_z and h_x, together with the requirement that e_z and h_x be continuous across the specimen faces, suffices to fix the amplitudes of the reflected and transmitted microwave fields. For the present application we are interested in the thick slab limit for which the amplitude of the transmitted microwaves becomes negligibly small.

For the thick slab limit one can set $e_z(d)=0$ and obtain

$$h_o=\left[\frac{ic}{\omega d}\right]\frac{e_z(o)}{[1+4\pi\chi_{xx}(o)]}\ , \tag{28a}$$

$$h_n=\frac{(2c/\omega d)(d/\delta)^2 e_z(o)}{\{(n\pi)^2-i(d/\delta)^2[1+4\pi\chi_{xx}(n)]\}}\ , \tag{28b}$$

from which

$$Z^{-1}=\frac{h_x(o)}{e_z(o)}=\left[\frac{2c}{\omega d}\right]\left[\frac{(i/2)}{[1+4\pi\chi_{xx}(o)]}+\left[\frac{d}{\delta}\right]^2\sum_{n=1}^{\infty}\frac{1}{\{(n\pi)^2-i(d/\delta)^2[1+4\pi\chi_{xx}(n)]\}}\right]\ , \tag{29}$$

where Z is the surface impedance of the metal, and where $\delta^2=c^2/4\pi\omega\sigma$, a quantity related to the classical skin depth. In terms of the surface impedance, the amplitude of the reflected microwaves is given by

$$h_R=\left[\frac{1-Z}{1+Z}\right]h_o\ , \tag{30}$$

and the fraction of the incident microwave power which is absorbed in the specimen is

$$\alpha=1-\left[\left|\frac{1-Z}{1+Z}\right|\right]^2\ . \tag{31}$$

For large wave numbers the susceptibility becomes very small because of the exchange terms in the resonant denominators of the susceptibility expressions:

$$\chi_{xx}\to M_s^2/2Ak^2\ , \tag{32a}$$

$$\chi_{yx}\to i(\omega/\gamma)(M_s)^3/(2Ak^2)^2\ . \tag{32b}$$

The limiting forms of these susceptibilities will not be altered by the presence of two-magnon scattering. It follows that the sum in Eq. (29) converges like $(n\pi)^{-2}$—a convergence which is too slow for a practical numerical calculation. It is useful to speed up convergence by adding and subtracting the sum

$$\sum_{n=1}^{\infty}\frac{1}{(n\pi)^2}=\tfrac{1}{6}$$

to obtain

$$Z^{-1}=\left[\frac{2c}{\omega d}\right]\left[\frac{i}{2[1+4\pi\chi_{xx}(o)]}+\frac{1}{6}\left[\frac{d}{\delta}\right]^2+i\left[\frac{d}{\delta}\right]^4\sum_{n=1}^{\infty}\frac{[1+4\pi\chi_{xx}(n)]}{(n\pi)^2\{(n\pi)^2-i(d/\delta)^2[1+4\pi\chi_{xx}(n)]\}}\right]\ . \tag{33}$$

The sum in (33) converges like $(n\pi)^{-4}$, which is sufficiently rapid for a practical computer calculation. In fact, for the cases treated in a later section of this paper we used a slab thickness of 10^{-3} cm and summed over 1000 terms. Extending the sum in (33) to 2000 terms did not change the calculated absorption by more than 1 part in 10^7.

Readers familiar with the Rado-Weertman formalism[2] will have noticed that no mention has been made of surface pinning in the above calculation. In adopting the form Eq. (26a) for $h_x(y)$, a cosine series, and by not explicitly introducing terms to represent effective surface fields, we have tacitly produced a solution corresponding to free surface spins, $dm_x/dy=dm_y/dy=0$. This can be seen by examining the series for the magnetization derivatives for small y (large n): both derivatives are proportional to y for very small y, and therefore vanish at the slab surface.

A solution for pinned spins can be obtained starting from Fourier series expansions

$$h_x(y)=\sum_{n=1}^{\infty}h_n\sin\left[\frac{n\pi y}{d}\right]\ , \tag{34a}$$

$$m_x(y)=\sum_{n=1}^{\infty}\chi_{xx}(n)h_n\sin\left[\frac{n\pi y}{d}\right]\ , \tag{34b}$$

and

$$e_z(y)=e_o+\sum_{n=1}^{\infty}e_n\cos\left[\frac{n\pi y}{d}\right]\ . \tag{34c}$$

For this case one obtains for the surface impedance, in the thick slab limit,

$$Z=\frac{e_z(o)}{h_x(o)}=\frac{c}{4\pi\sigma d}-\frac{i\omega d}{3c}-\left[\frac{2i\omega d}{c}\right]\sum_{n=1}^{\infty}\left[\frac{\mu(n)[(n\pi)^2+i(d/\delta)^2]-(n\pi)^2}{(n\pi)^2[(n\pi)^2-i(d/\delta)^2\mu(n)]}\right]\ , \tag{35}$$

where the sum $\sum_{n=1}^{\infty}1/(n\pi)^2=\frac{1}{6}$ has been added and subtracted to the Fourier series for $e_z(o)$ in order to obtain a rapidly converging series in the limit of large $(n\pi)$. In Eq. (35)

$$\mu(n)=1+4\pi\chi_{xx}(n)\ \text{and}\ \delta^2=c^2/4\pi\omega\sigma\ .$$

It can be demonstrated that m_x,m_y are proportional to y for small y and therefore that the transverse magnetization vanishes at the slab surface.

It would not be difficult to take arbitrary surface pinning into account. Consider a surface pinning energy of the form

$$E_s = E_o - \frac{K_1}{M_s^2} m_{xo}^2 - \frac{K_2}{M_s^2} m_{yo}^2 , \tag{36}$$

where m_{xo}, m_{yo} are the values of the rf magnetization at the front surface, $y=0$. This surface energy corresponds to surface magnetic fields of the form

$$h_x^s = -\frac{\partial E_s}{\partial m_{xo}} = \frac{2K_1}{M_s^2} m_{xo} \delta(y) , \tag{37a}$$

$$h_y^s = -\frac{\partial E_s}{\partial m_{yo}} = \frac{2K_2}{M_s^2} m_{yo} \delta(y) . \tag{37b}$$

These fields can be expanded in Fourier series and used as additional driving fields for the magnetization components

$$m_x(n) = \chi_{xx}(n)[h_n + h_x^s(n)] + \chi_{xy}(n) h_y^s(n) , \tag{38a}$$

$$m_y(n) = \chi_{yx}(n)[h_n + h_x^s(n)] + \chi_{yy}(n) h_y^s(n) , \tag{38b}$$

where the additional wave-number-dependent susceptibilities $\chi_{yy}(n)$ and $\chi_{xy}(n)$ can be calculated using an obvious extension of the formalism described in the previous sections. The coefficients $h_x^s(n)$ and $h_y^s(n)$ are the Fourier coefficients of h_x^s and h_y^s. The formalism for arbitrary surface pinning becomes, obviously, much more complicated than the calculation for the simple cases of free or completely pinned surface spins, and will not be pursued further.

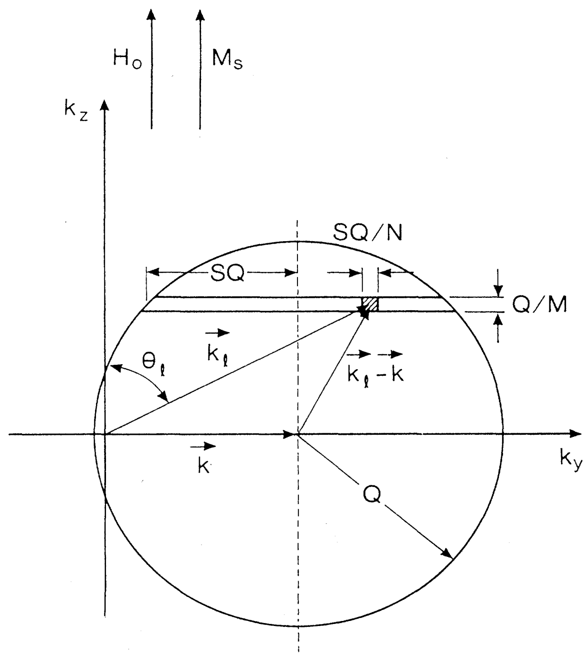

FIG. 2. The geometry used to calculate the wave-number-dependent susceptibilities corresponding to wave vector **k** in the presence of two-magnon scattering. The scattering amplitude for scattering from **k** to $\mathbf{k}_l$ is taken to be nonzero only if $(\mathbf{k}_l - \mathbf{k})$ lies within the sphere of radius Q cm^{-1} centered on the point defined by **k**. The sums which enter the expression for the susceptibility [Eqs. (24)] were calculated by summing contributions from stripes of constant angle θ, with respect to the K_z axis: these strips were Q/M thick and SQ/N wide, where $M=200$, $N=100$.

V. NUMERICAL CALCULATION OF THE SUSCEPTIBILITY

The scattering sums which appear in Eqs. (22) were calculated using a model in which the scattering amplitudes were assumed to be different from zero only if the scattered wave vector $\mathbf{k}_l$ lay within a sphere of radius Q centered on the wave vector **k** corresponding to the driving field $h_x = e^{i(ky-\omega t)}$, i.e., the scattering amplitudes were taken to be zero for $|\mathbf{k}-\mathbf{k}_l| > Q$, see Fig. 2. This model is a crude one, but it is tractable and a reasonable simulation of a collection of similar but independent scattering centers all of which have dimensions of order $2\pi/Q$ cm. Calculations were carried out using the following expressions for the scattering amplitudes, where the f's are adjustable constants:

(1) Exchange scattering:

$$F_{k,l} = f_e \mathbf{k}\cdot\mathbf{k}_l , \quad R_{k,l} = 0 ; \tag{39a}$$

(2) Anisotropy scattering:

$$F_{k,l} = R_{k,l} = f_a ; \tag{39b}$$

(3) Magnetization inhomogeneities:

$$F_{k,l} = f_m(3\cos^2\theta_l - 1) , \quad R_{k,l} = 0 . \tag{39c}$$

The amplitude parameters f_e, f_a, and f_m were adjusted to obtain the required linewidth at a particular frequency—usually 73 GHz, the highest experimental frequency available to us. They are related to the difference in magnetic properties between the scattering volume and the bulk through the expressions given in Eqs. (9), (10), and (11).

For each value k, the sums in Eqs. (22) were carried out by a numerical integration over the sphere of radius Q centered on the wave vector **k** (see Fig. 2) using the usual weighting factor $1/(2\pi)^3$ to account for the density of states in k space corresponding to a unit volume of magnetic material. The integration consisted of the sum over slices Q/M thick parallel to the k_x-k_y plane; within such a slice, contributions from strips corresponding to θ=const, and of width SQ/N, were added together. The integration over the angle ϕ could be carried out analytically. For most of the calculations we used $M=200$, $N=100$, and $Q=1.0\times10^6$ cm^{-1} as a reasonable compromise between the desire to obtain numerical credibility and the need to keep computation times within reasonable bounds. Moreover, this value of Q is comparable to the width of the magnon manifold in k space for a material characterized by $4\pi M_s = 16.7$ kOe ($\Delta k \sim 2\times 10^6$ cm^{-1}). The time required to calculate the susceptibilities for each value of k was 3.3 sec on an IBM 30816X computer; this time increased approximately as the square of Q. In order to calculate the surface impedance of the metal, and hence its absorption, from Eq. (31), it is necessary to know the value of the susceptibility on an equally spaced grid of approximately 1000 wave numbers: in the sum over $k = n\pi/d$ we used $d = 10^{-3}$ cm, and a sum running up to $n = 1000$. It would require a prohibitively long computing time to calculate the susceptibility for each value of k: at 3.3 sec per value of k, each magnetic field value would require 55 min of CPU time. We therefore calculated the sums used to obtain the susceptibility [i.e., the sums in Eqs. (22)] on a grid of up to forty values of k equally spaced over the interval $0-Q$ cm^{-1}. A linear interpolation was used to obtain the required sums for values of k not on the grid points: fortunately, the variation of the sums with wave number for fields near ferromagnetic resonance was found to be relatively smooth. For values of k greater than Q cm^{-1} the sums were held fixed at their values corresponding to $k = Q$ cm^{-1}. This arbitrary cutoff at large values of k introduced very little error because the sum in Eq. (29) for the surface impedance converges so rapidly that the terms for $k > 1.0\times 10^6$ make very little contribution to the total. For example, doubling the number of terms to $n = 2000$ changed the surface impedance by less than 1 part in 10^7 using $Q = 10^6$ cm^{-1} for a typical case ($Fe_{82}B_{18}$ at 80 GHz and for exchange scattering).

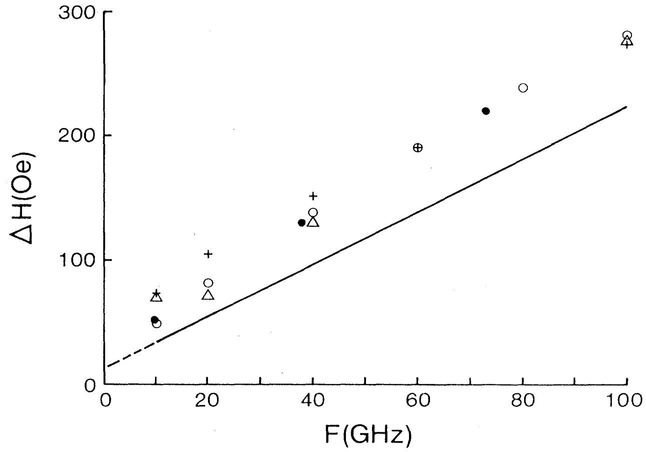

FIG. 3. The results of linewidth calculations for $Fe_{82}B_{18}$. The measured linewidths[8] are indicated by the solid points (●). Exchange inhomogeneity scattering is denoted by ○, using $f_e = 5.6\times 10^{-17}$ [see Eq. (39a)]. Anisotropy inhomogeneity scattering is denoted by +, using $f_a = 1.6\times 10^{-6}$ [see Eq. (39b)]. Magnetic inhomogeneity scattering is denoted by △, using $f_m = 2.6\times 10^{-6}$ [see Eq. (39c)]. The scattering amplitudes f_i were adjusted to give the experimental linewidth at 73 GHz. The solid line is the frequency dependence of the linewidth calculated for no two-magnon scattering and no pinning using the Landau-Lifshitz damping parameter G, measured by means of FMAR transmission experiments. Parameters used in the calculations were $4\pi M_s = 16.67$ kOe, $G = 1.0\times 10^8$ Hz, $g = 2.08$, $A = 0.84\times 10^{-6}$ ergs/cm, and $R = 135.0\times 10^{-6}$ Ω cm.

VI. RESULTS

The results of FMR linewidth calculations using parameters[6,27] appropriate for amorphous $Fe_{82}B_{18}$, and no surface pinning, are shown in Fig. 3, along with experimentally measured linewidths. The scattering strengths, f_e, f_a, and f_m of Eqs. (39), were chosen so that the calculated and observed linewidths agreed at 73 GHz using an intrinsic damping parameter $G = 1.1\times 10^8$ Hz. The intrinsic damping parameter was measured using the ferromagnetic antiresonance (FMAR) transmission technique[3]; two-magnon damping plays no role in this method because at antiresonance, $\omega/\gamma = B$, the signal frequency lies well above the frequencies in the magnon manifold so that the density of final states available for scattering becomes very small. The solid line in Fig. 3 presents the results of the linewidth calculation for no two-magnon scattering. This case should be a reasonable test of the first-order perturbation calculation since the additional linewidth due to two-magnon scattering is less than the intrinsic linewidth for frequencies greater than 10 GHz. As can be seen from the figure, the calculated linewidths track the experimentally observed linewidths for the three scattering mechanisms considered. This is a bit disappointing, for we had hoped that the frequency dependence of the two-magnon contribution would give some clue as to the nature of the scattering centers.

The scattering amplitudes used to obtain the calculated points shown in Fig. 3 for exchange and anisotropy scattering are large in the sense that they demand a relatively large difference in magnetic properties between the inhomogeneity and the matrix material. This can be seen as follows. Let each inhomogeneity be a sphere of radius $R = 2\pi/Q = 2\pi\times 10^{-6}$ cm for $Q = 1.0\times 10^6$ cm^{-1}. Such a region has a volume $v = 1.0\times 10^{-15}$ cm^3. The maximum concentration of such regions is $N = (1/2R)^3 = 5\times 10^{14}$/cm^3. It is the square of the matrix elements which is proportional to N for independent scattering centers; the scattering amplitude to be associated with a single center is the total amplitude divided by $\sqrt{N}$. The exchange amplitude used to obtain the points in Fig. 3 was $f_e = 5.6\times 10^{-17}$. This corresponds to a discontinuity in the exchange stiffness parameter $\Delta A = 1.7\times 10^{-6}$ ergs/cm [from Eq. (9) and for $4\pi M_s = 16.7$ kOe]. This value is comparable with the exchange stiffness parameter characteristic of ferromagnetic metals ($\sim 10^{-6}$ ergs/cm). Similarly, one can estimate from (10), using the value $f_a = 1.6\times 10^{-6}$ for magnetic anisotropy scattering, that the discontinuity in magnetic anisotropy parameter between the inhomogeneity and the matrix must be at least $\Delta K = 4.8\times 10^4$ ergs/cm^3. This value can be compared with the cubic anisotropy for room-temperature iron, $K_1 = 4.8\times 10^5$ ergs/cm^3. On the other hand, the magnetic scattering amplitude, $f_m = 2.6\times 10^{-6}$, corresponds [from Eq. (11)] to a magnetization discontinuity $\Delta M_s = 12$ Oe.

On the basis of these crude estimates it appears that both the exchange scattering and magnetic anisotropy scattering mechanisms are too weak to account for the nonintrinsic FMR line broadening observed in $Fe_{82}B_{18}$. This conclusion is not sensitive to the choice of cutoff wave vector, Q. If one uses a cutoff wave number $Q=10^7$ cm^{-1}, the scattering amplitudes required to fit the data of Fig. 3 are $f_e=1.5\times10^{-18}$, $f_a=9.0\times10^{-7}$, and $f_m=9.5\times10^{-17}$. A repetition of the preceding estimates leads to the conclusion that the linewidths observed for $Fe_{82}B_{18}$, if due to two-magnon scattering, would require fluctuations in the exchange parameter at least as large as 1.4×10^{-6} ergs/cm, fluctuations in the anisotropy parameter at least as large as 9×10^5 ergs/cm^3, and fluctuations in the magnetization at least as large as 140 Oe. The fluctuations required for the exchange and anisotropy scattering mechanisms are both too large to be plausible.

It is an interesting fact that the variation with frequency of the linewidth due to exchange scattering can be reproduced by including a spin diffusion term in the Landau-Lifshitz equation of motion,[3] i.e.,

$$\frac{\partial \mathbf{m}}{\partial t} = -\gamma(\mathbf{M}\times\mathbf{H}_{\text{eff}}) + D\nabla^2\mathbf{m} + \text{damping term} . \quad (40)$$

In addition to the parameters listed in the caption of Fig. 3, we have used the formalism described by Cochran, Heinrich, and Dewar,[3] along with $D=0.22$ cm^2/sec and no pinning, to calculate the frequency dependence of the FMR linewidth. The resulting linewidths were the same as those calculated for two-magnon exchange scattering within 4 Oe except at the lowest frequency (10 GHz) for which the linewidth was calculated to be 42 Oe using diffusion versus 48 Oe calculated for the case of two-magnon exchange scattering. The equivalence of linewidths calculated using exchange scattering with those calculated using the diffusion term in the Landau-Lifshitz equation of motion is perhaps not so surprising since both the diffusion torques and the exchange scattering are proportional to the square of the wave number. This equivalence does, however, provide support for the basic correctness of our rather complex two-magnon scattering calculation. The addition of an imaginary component to the exchange stiffness parameter, A, would have much the same effect as adding a diffusion term to the Landau-Lifshitz equation of motion. It therefore seems very reasonable that the effect of fluctuations in the exchange coupling parameter should be describable in terms of an imaginary component of the effective exchange field: this imaginary component of the exchange field would then augment the ordinary Landau-Lifshitz damping field $(i\omega/\gamma)(G/\gamma M_s)$.

VII. CONCLUSIONS

In this paper we have used the two-magnon scattering mechanism to investigate the effect of magnetic inhomogeneities on the FMR linewidths of ferromagnetic metals. The wave-number- and frequency-dependent susceptibility was evaluated in the presence of two-magnon scattering: dipole-dipole interactions were included in the calculation of the susceptibility in order that the theory be applicable to materials having a large saturation magnetization. Spatial inhomogeneities in the magnetization distribution caused by eddy currents in a ferromagnetic metal were included in the solution of the combined Maxwell's and Landau-Lifshitz equations by expanding the magnetization components and the electromagnetic field components in Fourier series. In that way the two-magnon scattering mechanism, which is wave-number and frequency dependent, could be included self-consistently in the treatment of ferromagnetic resonance absorption in metals.

The simple theory presented here does seem to reproduce the main features of the excess FMR linewidth observed for many amorphous metal alloys; namely, an increase in linewidth over the intrinsic linewidth by an amount which is approximately frequency independent. Two-magnon scattering does, therefore, appear to offer an explanation for the source of a damping mechanism which broadens the FMR absorption line without affecting the damping as measured by FMAR transmission experiments.

Under conditions for which a first-order perturbation calculation is a reasonable approximation, two-magnon scattering should not contribute to FMR linewidths measured with the applied field normal to the specimen plane. This is a consequence of the fact that for magnon propagation along the magnetization, there are no resonant final states into which the magnons can be scattered. Unfortunately, it is not a simple matter to check this consequence of the theory. In the first place, FMR measurements at high frequencies for the field normal configuration require very large values of the external field: the applied field must exceed ω/γ by more than $4\pi M_s$. In the second place, the FMR linewidth in the field normal configuration is notoriously sensitive to surface irregularities, and therefore it is difficult to be certain that the observed linewidth is that characteristic of a smooth surface. Of course, inhomogeneous line broadening due to surface roughness is a consequence of a particular kind of two-magnon scattering process. However, it is not a two-magnon scattering process for which the simple model used above is appropriate.

ACKNOWLEDGMENT

The authors would like to thank the Natural Sciences and Engineering Research Council of Canada for the grants which partially supported this work.

[1]W. S. Ament and G. T. Rado, Phys. Rev. **97**, 1558 (1955).
[2]G. T. Rado and J. R. Weertman, J. Phys. Chem. Solids **11**, 315 (1959).
[3]J. F. Cochran, B. Heinrich, and G. Dewar, Can. J. Phys. **55**, 787 (1977).
[4]J. F. Cochran, K. Myrtle, and B. Heinrich, J. Appl. Phys. **53**, 2261 (1982).
[5]B. Heinrich, K. Myrtle, J. M. Rudd, J. F. Cochran, and R. Hasegawa, J. Magn. Magn. Mater. **31-34**, 1597 (1983).
[6]B. Heinrich, J. M. Rudd, K. Urquhart, K. Myrtle, J. F. Cochran, and R. Hasegawa, J. Appl. Phys. **55**, 1814 (1984).
[7]S. M. Bhagat, S. Haraldson, and O. Beckman, J. Phys. Chem. Solids **38**, 593 (1977).
[8]M. L. Spano and S. M. Bhagat, J. Magn. Magn. Mater. **24**, 143 (1981).
[9]L. Kraus, Z. Frait, and J. Schneider, Phys. Status Solidi A **63**, 669 (1981); **64**, 449 (1981).
[10]D. J. Webb and S. M. Bhagat, J. Magn. Magn. Mater. **42**, 109 (1984).
[11]S. M. Bhagat, D. J. Webb, and M. A. Manheimer, J. Magn. Magn. Mater. **53**, 209 (1985).
[12]T. D. Rossing, J. Appl. Phys. **34**, 995 (1963).
[13]C. E. Patton, C. H. Wilts, and Floyd B. Humphrey, J. Appl. Phys. **38**, 1358 (1967).
[14]B. Heinrich, K. B. Urquhart, A. S. Arrott, J. F. Cochran, K. Myrtle, and S. T. Purcell, Phys. Rev. Lett. **59**, 1756 (1987).
[15]B. Heinrich, K. B. Urquhart, J. R. Dutcher, S. T. Purcell, J. F. Cochran, and A. S. Arrott, J. Appl. Phys. **63**, 3863 (1988).
[16]A. Berteaud and H. Pascard, J. Appl. Phys. **36**, 970 (1965).
[17]A. M. Clogston, H. Suhl, L. R. Walker, and P. W. Anderson, J. Phys. Chem. Solids **1**, 129 (1956).
[18]M. Sparks, *Ferromagnetic Relaxation Theory* (McGraw-Hill, New York, 1964).
[19]E. Schlömann, J. Appl. Phys. **40**, 1199 (1969); Phys. Rev. **182**, 632 (1969).
[20]L. L. Hirst, Phys. Rev. **164**, 971 (1967).
[21]B. Heinrich, J. F. Cochran, and R. Hasegawa, J. Appl. Phys. **57**, 3690 (1985).
[22]E. A. Turov, in *Ferromagnetic Resonance,* edited by S. V. Vonsovskii (Pergamon, Oxford, 1966), p. 82.
[23]V. Kopsky, Czech. J. Phys. **B18**, 1094 (1968).
[24]M. Sparks, B. Loudon, and C. Kittel, Phys. Rev. **122**, 791 (1961).
[25]W. Schmidt, J. Phys. C **21**, 3533 (1988).
[26]D. N. Zubarev, Usp. Fiz. Nauk. **71**, 71 (1960) [Sov. Phys. Usp. **3**, 320 (1960)].
[27]J. J. Rhyne, G. E. Fish, and J. W. Lynn, J. Appl. Phys. **53**, 2316 (1982).